Atmos. Meas. Tech. Discuss., https://doi.org/10.5194/amt-2018-61
Manuscript under review for journal Atmos. Meas. Tech.
Discussion started: 19 April 2018

Atmospheric Measurement Techniques Discussions

Measuring turbulent CO_2 fluxes with a closed-path gas analyzer in marine environment

Martti Honkanen[1], Juha-Pekka Tuovinen[2], Tuomas Laurila[2], Timo Mäkelä[2], Juha Hatakka[2], Sami Kielosto[1,3], and Lauri Laakso[1,4]

[1]Meteorological and Marine Research Programme, Finnish Meteorological Institute, Finland
[2]Climate Research Programme, Finnish Meteorological Institute, Finland
[3]Marine Ecology Research Laboratory, Finnish Environment Institute, Finland
[4]School of Physical and Chemical Sciences, North-West University, Potchefstroom Campus, South Africa

Correspondence: Martti Honkanen (martti.honkanen@fmi.fi)

Abstract. Sea-air fluxes of carbon dioxide (CO_2) were measured using the eddy covariance method at a new station established on the Utö island in the Baltic Sea. The flux measurement system is based on a closed-path infrared gas analyzer (LI-7000, LI-COR) requiring only occasional maintenance, so the station is capable of continuous monitoring. However, such infrared gas analyzers are prone to significant water vapor interference in a marine environment, where CO_2 fluxes are small.

In July–October 2017, two LI-7000 analyzers were run in parallel to test the effect of a sample air drier which dampens water vapor fluctuations, and a virtual impactor, included to remove liquid sea spray, both of which were attached to the sample air tubing of one of the analyzers. The systems showed closely similar ($R^2 = 0.99$) sea-air CO_2 fluxes when the latent heat flux was low, which proved that neither the drier nor the virtual impactor perturbed the CO_2 flux measurement. However, the undried measurement had a positive bias that increased with increasing latent heat flux, suggesting water vapor interference.

For both systems, cospectral densities between vertical wind speed and CO_2 were distributed within the expected frequency range, with a moderate attenuation of high-frequency fluctuations. While the setup equipped with a drier and a virtual impactor generated a slightly higher flux loss, we opt for this alternative for its reduced water vapor cross-sensitivity and better protection against sea spray. The integral turbulence characteristics were found to agree with the universal stability dependence observed over land. Non-stationary flow conditions caused unphysical results, which resulted in a high percentage (up to 63 %) of discarded measurements. After removing the non-stationary cases, the direction of the sea-air CO_2 fluxes was in good accordance with the measured CO_2 partial pressure difference between the sea and the atmosphere. Atmospheric CO_2 concentration changes larger than $2\,\mathrm{ppm}$ during a $30\,\mathrm{min}$ averaging period were found to be associated with the non-stationarity of CO_2 fluxes.

The Utö Atmospheric and Marine Research Station continues to monitor the regional CO_2 exchange between the sea and the atmosphere, utilizing the results of this work.

Atmos. Meas. Tech. Discuss., https://doi.org/10.5194/amt-2018-61
Manuscript under review for journal Atmos. Meas. Tech.
Discussion started: 19 April 2018

Atmospheric Measurement Techniques Discussions

1 Introduction

Anthropogenic actions, such as combustion of fossil fuels and land use changes, have perturbed the global carbon cycle, resulting in climatic changes (e.g. Solomon et al., 2009). A quarter of the anthropogenic carbon dioxide (CO_2) emissions to the atmosphere are bound by the oceans (Heinze et al., 2015), causing ocean acidification (Feely et al., 2009). To better understand the global carbon cycle, measurements of the CO_2 exchange between the atmosphere and marine ecosystems are required. These measurements are also useful for developing parameterizations of gas exchange intensity, such as the gas transfer velocity, used in global carbon models (e.g. Takahashi et al., 2002). In the case of coastal seas, sea-air CO_2 flux measurements provide information about the feedbacks between the aquatic carbonate system and marine ecosystems, since the direction and magnitude of these fluxes depend on the photosynthetic carbon assimilation in surface seawater. Although the continental margin seas cover only a small portion of the oceans, up to 15 % of the total ocean primary production takes place in these seas, which are responsible for over 40 % of the total oceanic carbon sequestration (Muller-Karger et al., 2005).

With the development of fast-response infrared CO_2 analyzers, it has become possible to apply the eddy covariance method for directly measuring the sea-air CO_2 fluxes (Jones and Smith, 1977). Early on, however, Webb et al. (1980) showed that the CO_2 flux measurements made with this technique need to be corrected for the effects of temperature and water vapor (H_2O) fluctuations. This correction can be significant in aquatic environment, even of the same order as the measured CO_2 flux (Sahlée et al., 2011). More recently, it has been recognized that CO_2 gas analyzers suffer from water vapor cross-sensitivity (Kohsiek, 2000). Blomquist et al. (2014) concluded that this is the most significant error source in sea-air CO_2 flux measurements, because the CO_2 fluxes in marine environment are typically small, as compared to terrestrial ecosystems. A solution to the cross-sensitivity problem is to dry the sample air before the measurement (e.g. Miller et al., 2010). Also, efforts have been made to correct for the cross-sensitivity problem in the data post-processing phase (e.g. Prytherch et al., 2010; Edson et al., 2011). However, these corrections may be inadequate and thus do not obviate the use of a drier (Landwehr et al., 2014).

The cross-sensitivity results from the overlap of the infrared radiation frequency bands of CO_2 and H_2O, because of which the H_2O molecules present will increase the apparent CO_2 concentration. If the optical filter, used for the selection of the transmitted frequency band, leaks out-of-band radiation, a substance with a different absorption frequency band can interfere the measurement. This effect is referred to as the direct absorption cross-sensitivity. In addition, the collisions with different molecules cause the frequency bands to broaden (so-called pressure broadening). By testing some commercial infrared gas analyzers, Kondo et al. (2014) found out that the factory-calibrated correction for the direct absorption interference may not be optimized and that the pressure broadening effect caused an overestimation of the CO_2 flux, which increased with increasing water vapor flux.

Infrared gas analyzers are classified according to the type of the optical path: the open-path analyzers measure the absorption of the infrared signal in ambient air, whereas the closed-path gas analyzers have an enclosed measurement chamber. Both types suffer from H_2O cross-sensitivity but otherwise have differing pros and cons; for instance, the closed-path instruments are known to act as low-pass filters, which generates a loss in the measured flux (Leuning and King, 1992). On the other hand, a long sample line attenuates temperature fluctuations, thus eliminating the need for correcting for sample air expan-

Atmos. Meas. Tech. Discuss., https://doi.org/10.5194/amt-2018-61
Manuscript under review for journal Atmos. Meas. Tech.
Discussion started: 19 April 2018

Atmospheric Measurement Techniques Discussions

sion/contraction (Rannik et al., 1997). For a closed-path analyzer, the dilution due to water vapor (Webb et al., 1980) can be corrected accurately as a point-by-point operation on the high frequency data, which is not possible with open-path analyzers (Ibrom et al., 2007).

As direct sea-air gas exchange measurements are performed in the surface boundary layer, in a close proximity to the water surface, liquid sea spray may block the optical path of open-path sensors and clog the inlet of closed-path analyzers. In addition, high relative humidity can produce H_2O condensation on the lenses of an open-path system. In a closed-path system, the accumulation of sea salt on the optical lenses is minimized as the inlet is typically protected by a Teflon filter. Efforts have been made to solve the sea-spray contamination problem of open-path sensors by cleaning the optics regularly (Kondo and Tsukamoto, 2007). However, this may be technically challenging, because sea salt films can be formed on the windows of an open-path analyzer in a matter of hours (Miller et al., 2010).

Open-path gas analyzers have been mostly applied for sea-air CO_2 flux measurements due to their low power consumption, small high frequency attenuation and ease of data synchronization with wind measurements (Blomquist et al., 2014). Additionally, Miller et al. (2010) found out that closed-path sensors are more sensitive to (ship) motion than the open-path sensors.

While the eddy covariance method is widely used for directly measuring the surface-atmosphere exchange of energy and matter, it is based on several theoretical assumptions. These include the horizontal homogeneity of terrain and the stationarity of transport processes, and that turbulence is fully developed and there exists no other transport mechanisms than vertical turbulence (e.g. Dabberdt et al., 1993). Foken and Wichura (1996) noted that flow non-stationarity is one of the most serious problems affecting the surface exchange measurements, as in such conditions the observed turbulent flux does not equal the flux at the surface. The stationarity assumption can be violated owing to diurnal forcings and varying weather patterns, for example.

The Baltic Sea forms a large and diverse biogeochemical system, providing a great potential for studying interactions between the marine ecosystem and the aquatic carbonate system. However, only a few fixed measurement sites measuring sea-air CO_2 fluxes are located in the Baltic Sea (Rutgersson et al., 2008; Lammert-Stockschaeder and Ament, 2015). A micrometeorological tower placed on the shore of an island offers a cost-effective alternative to ship measurements, as maintenance and installations are more effortless. Moreover, a motion correction, required with ship measurements, is not needed and the flow distortion can be minimized with a suitable positioning of the flux tower.

In this paper, we introduce a newly established and currently operating eddy covariance measurement site, located on the Utö island in the Baltic Sea, and analyze empirically the effect of water vapor on the CO_2 sea-air fluxes. After experimenting with an open-path and a semi-open-path gas analyzer, we opted for a closed-path sensor, which can be protected against sea spray contamination, and the drying of sample air is straightforward to implement. We compare measurements made with two identical closed-path analyzers, one of which is equipped with a drier and a virtual impactor. We also address the quality of these measurements by analyzing the stationarity and integral turbulence characteristics of the flow and the homogeneity of flux footprints.

Atmos. Meas. Tech. Discuss., https://doi.org/10.5194/amt-2018-61
Manuscript under review for journal Atmos. Meas. Tech.
Discussion started: 19 April 2018

Atmospheric Measurement Techniques Discussions

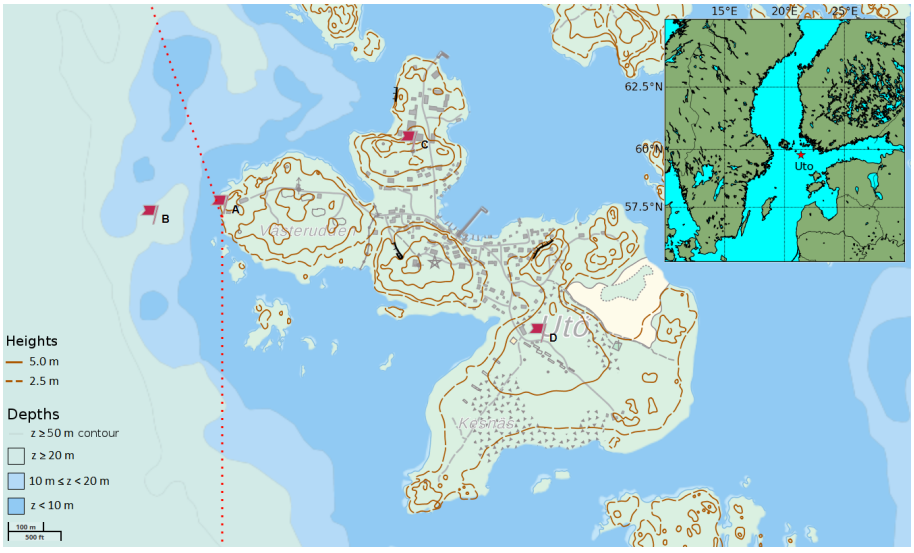

Figure 1. Location of the Utö island in the Archipelago Sea. The research installations on the island consist of the Utö Atmospheric and Marine Research Station (A), a flow-through pumping system (inlet at B), the Atmospheric ICOS station (C), and a weather and air quality station (D). The red dashed lines indicate the wind sector suitable for sea-air flux measurements (180–340°).

2 Materials and methods

2.1 Site description

The measurement site is located on the island of Utö in the southern edge of the Archipelago Sea in the Baltic Sea (59°46'55" N, 21°21'27" E) (Fig. 1). The Archipelago Sea is a small sea area between the southwest coast of Finland and the sea of Åland and is characterized by thousands of small islands. The island of Utö is a treeless cliff with small shrubs, with an area of 0.81 km^2 .

Since 2012, the Finnish Meteorological Institute has been building up the new Utö Atmospheric and Marine Research Station in collaboration with the Finnish Environment Institute. The choice of this island was due to its easy access, well-developed technical infrastructure, permanent inhabitation and the long-term meteorological and marine measurements. Finnish Meteorological Institute's meteorological measurements date back to 1881, and the seawater temperature and salinity measurements were initiated in 1900 (Laakso et al., 2018). Also, the Integrated Carbon Observation System (ICOS) research infrastructure has an atmospheric station on the island.

The Utö Atmospheric and Marine Research Station and its flux tower are located on the western side of the island. To the west of the shore, the water depth quickly deepens to 80 m. The closest shoal, Tratten, is located 1.4 km to the southwest and has an area of 0.6 hectares.

Atmos. Meas. Tech. Discuss., https://doi.org/10.5194/amt-2018-61
Manuscript under review for journal Atmos. Meas. Tech.
Discussion started: 19 April 2018

Figure 2. The flux tower on the shore of the Utö island during a high western swell (photo by Ismo Willström).

The mean annual wind speed at Utö is 7.1 $\mathrm{m\,s^{-1}}$. On average, the minimum monthly wind speed occurs in July (5.6 $\mathrm{m\,s^{-1}}$) and the maximum in December (8.9 $\mathrm{m\,s^{-1}}$). The wind blows approximately 60 % of the time from the sector between south and northwest (Fig. 1), providing a good temporal coverage for the sea-air flux measurements. (Pirinen et al., 2012)

The mean annual air temperature in Utö is 6.6 °C, whereas the mean annual surface seawater temperature at the depth of 5 m is 8.1 °C. In deep water (at 50 m depth), the mean annual seawater temperature is 4.4 °C. The maximum monthly mean air temperature (16.7 °C) is observed in July, whereas the seawater at 5 m depth reaches its maximum temperature (16.1 °C) in August. The minimum temperature of air (-2.1 °C) occurs in February, while the temperature of the surface seawater is at its minimum (1.0 °C) in March. On average, there exists ice around Utö for every few years with a typical ice cover duration ranging from one to three months. (Laakso et al., 2018)

Unlike the oceans, the carbon cycle in the Baltic sea is heavily influenced by biological activity. During summer, the partial pressure of CO_2 (pCO_2) in surface water declines to approximately 15 Pa as a result of primary production. pCO_2 in surface water has its maximum (60 Pa) during winter, when biological activity is diminished, mineralization prevails and mixing processes transport CO_2-rich seawater to the surface. Due to the annual cycle of primary production, the Baltic Sea is a source of CO_2 to the atmosphere in winter and a sink in summer. Upwelling and diurnal biological cycle generate short-term variations in the surface water pCO_2. (Wesslander, 2011)

2.2 Instrumentation

A 9 m tall micrometerological tower is placed on the western shore of the island (Figs. 1, 2). The tower is mounted on a cliff that has no vegetation. The base of the tower is approximately 3 m above the sea level and the horizontal distance between the tower and the sea is approximately 4 m. When measuring sea-air exchange, only the fluxes related to the westerly winds (180–340°) are used.

Atmos. Meas. Tech. Discuss., https://doi.org/10.5194/amt-2018-61
Manuscript under review for journal Atmos. Meas. Tech.
Discussion started: 19 April 2018

Atmospheric Measurement Techniques Discussions

Air velocity components together with air temperature, T, were measured with an acoustic anemometer/thermometer (uSonic-3, Metek) attached to the top of the tower (11.5 m a.s.l.). CO_2 and H_2O molar fractions were measured by using two closed-path differential non-dispersive infrared gas analyzers (LI-7000, LI-COR) that were placed in a 1.5 m tall instrument hut close to the tower (Fig. 2). The inlets of both sample flows are protected with a grate and are located directly beneath the anemometer; the distance between the inlets and the lower anemometer transducers is 30 cm. The outside parts of the tubes are approximately 10 m long and are made of Teflon (inner diameter of 3.175 mm) and steel (inner diameter of 4.0 mm). The steel-tube sample line is equipped with a virtual impactor (see Appendix), to protect the instrument from possible exposure to liquid water, and a 30 cm long PD-100T-12-MKA drier (Perma-Pure) to attenuate water vapor fluctuations. The drier is based on the partial pressure difference that drives water vapor from the sample air to the purge stream through a Nafion membrane. Nafion driers are found to have only a small permeability to CO_2 (Welp et al., 2013).

Inside the instrument hut, the flow continues in 1 m long Bev-A-Line tubes, which are protected by Teflon filters and connected to the analyzers. Data are logged at a 10 Hz frequency and transmitted through the Internet to a server. The hut temperature is regulated using a fan and a radiator, since large temperature changes influence the performance of the CO_2 analyzers.

An external pump is used for producing a sample flow at a rate of approximately $6\,\mathrm{l\,min^{-1}}$ for both setups. We operate the LI-7000 gas analyzers in the absolute mode, which means that a small stream of zero gas (0 ppm CO_2) is constantly flowing through the reference cell of both analyzers. The gas analyzers are calibrated with zero and span (364.4 ppm CO_2) gases every three months. After calibration, the Teflon filters are renewed and the virtual impactor is cleaned. The outside tubes are washed with an isopropyl alcohol-water mixture annually. At the same time, the Bev-A-Line tubes and the internal chemicals of the gas analyzers are renewed and the optical paths are cleaned.

The setup with the Nafion drier and the virtual impactor is referred here to as the 'test setup' and the other setup as the 'standard setup'. The standard setup represents a typical closed-path gas analyzer-based eddy covariance setup commonly applied on terrestrial ecosystems (e.g. Aurela et al., 2015). The test setup is an improved version of this configuration, designed especially for a marine environment where water vapor and sea spray are likely to give rise to problems.

2.3 Methods used in flux calculations

As the LI-7000 gas analyzer does not directly provide molar fractions with respect to dry air, we first calculated the dilution corrected CO_2 molar fraction as:

$$c = \frac{c_w}{1-q}, \tag{1}$$

where c_w is the uncorrected molar fraction of CO_2 and q is the molar fraction of H_2O.

It is assumed that the long pipe lines, both Teflon and steel, strongly attenuate the temperature fluctuations and thus there is no need for correcting for expansion/contraction effects in the sample air (Rannik et al., 1997). The eddy covariance mass flux was calculated from the fluctuations of molar fractions of an atmospheric quantity, χ, and vertical wind speed, w:

$$F = \rho_d \overline{w'\chi'}, \tag{2}$$

Atmos. Meas. Tech. Discuss., https://doi.org/10.5194/amt-2018-61
Manuscript under review for journal Atmos. Meas. Tech.
Discussion started: 19 April 2018

Atmospheric Measurement Techniques Discussions

where ρ_d is the dry air density. The primes denote the 10 Hz fluctuations with respect to a time average and the overbar denotes arithmetic averaging. An averaging period of 30 min was adopted. For each period, the time delay between the acoustic anemometer and gas analyzer data flows was determined by maximizing the (absolute) covariance in Eq. 2 within a predefined time window, and a double coordinate rotation was applied to ensure zero vertical wind speed.

Obvious outliers were discarded by including only those CO_2 fluxes that are within three standard deviations from the mean. The fulfillment of several theoretical requirements for the eddy covariance measurements was considered. The non-stationarity of the flux measurements was analyzed by comparing the average of the CO_2 fluxes calculated for 5 min subperiods ($\frac{1}{6}\sum_{i=1}^{6}\overline{w'c'}_{5\,\mathrm{min,\,i}}$, where i is the index of the subperiod) with the 30 min flux ($\overline{w'c'}_{30\,\mathrm{min}}$) (Foken and Wichura, 1996). The relative non-stationarity, RN, for a given variable, ζ, was defined as:

$$RN_{\zeta} = \left| \frac{\frac{1}{6}\sum_{i=1}^{6}\zeta_{5\,\mathrm{min,\,i}} - \zeta_{30\,\mathrm{min}}}{\zeta_{30\,\mathrm{min}}} \right|. \quad (3)$$

In the case of CO_2 flux, $\zeta = \overline{w'c'}$. To test the development of turbulence, integral turbulent characteristics of temperature and vertical velocity were compared to universal surface-layer functions (Thomas and Foken, 2002). It is assumed that turbulent transport of all scalars (T, CO_2 and H_2O) are similar, and thus only the characteristics of T are examined here. For this examination, only stationary flow conditions ($RN_{\overline{w'c'}} < 0.3$) within the sea sector are included. An observation is also discarded if a positive momentum flux is measured, as these can be considered a sign of flow non-stationarity (Yang et al., 2016).

2.3.1 Spectral analysis

High frequency attenuation was examined by calculating the cospectra between w and c ($Co_{w\mathrm{CO_2}}$) and q ($Co_{w\mathrm{H_2O}}$) and comparing these with the corresponding cospectra between w and T (Co_{wT}). For this purpose, it is assumed that the high frequency end of Co_{wT} is unattenuated and the atmospheric turbulent transport of heat, water vapor and CO_2 are similar.

Before calculating the half-hourly cospectra using the discrete Fourier transfrom, the 10 Hz data were linearly detrended and the Hamming window was applied. The cospectra were normalized with the corresponding covariances and interpolated into 64 logarithmically equally spaced bins.

Observations with an appropriate wind direction (180–340°) and stationary flow conditions, based on the criterion that $RN_{\overline{w'c'}} < 0.3$, were accepted for spectral analysis. Observations during slightly unstable to slightly stable hydrostatic stability conditions ($|z/L| < 0.05$) were examined, where z is the measurement height and L is the Obukhov length. In total, 612 observations met these criteria. Furthermore, every cospectrum was visually inspected and the clearly distorted ones (365) were discarded. Thus, 247 observations from a 4 month period were used for the spectral analysis.

To describe the spectral attenuation of the flux as a function of frequency, f, a transfer function, Γ, was determined. For fitting the transfer function, the cospectra were normalized so that their peaks were leveled. Also, the outermost points were discarded. Using a non-linear least squares fit, an exponential transfer function was fitted to the ratio of $Co_{w\mathrm{CO_2}}$ or $Co_{w\mathrm{H_2O}}$ to Co_{wT}:

$$\Gamma(f) = \exp[-\log(2)(\frac{f}{f_0})^2], \quad (4)$$

Atmos. Meas. Tech. Discuss., https://doi.org/10.5194/amt-2018-61
Manuscript under review for journal Atmos. Meas. Tech.
Discussion started: 19 April 2018

where f_0 is the half-power frequency at which the ratio of cospectral densities is 0.5. In the case of H_2O fluxes, a power-law relationship between f_0 and relative humidity (RH) was additionally derived similarly to Mammarella et al. (2009).

To correct for the high-frequency attenuation of fluxes, which depends on stability and wind speed, the universal Co_{wT} equations reformulated by Horst (1997) from those originally presented by Kaimal et al. (1972) and Kaimal and Finnigan (1994) were used as a reference.

2.4 Auxiliary data

In addition to the flux measurements, we present here data of the dissolved CO_2 concentration in surface seawater, which is monitored using a SuperCO$_2$ system (Sunburst Sensors) connected to a flow-through pumping system. The SuperCO$_2$ instrument consists of a shower-head equilibration chamber and an infrared gas analyzer (840A, LI-COR). To account for sensor drift, the flows of four reference gases are directed into the instrument every four hours, and a linear correction is calculated from these calibration measurements. The system automatically cleans the equilibration chamber with hydrogen peroxide periodically. The inlet for seawater intake is located 250 m west of the station (Fig. 1) and it is kept at 5 m depth by using floats. The water depth at this location is 23 m. Since sample water exchanges heat with the pipe and its surroundings, a correction for this temperature effect was applied according to Takahashi et al. (1993):

$$\mathrm{pCO_{2_{in}}} = \mathrm{pCO_{2_{eq}}} \exp[0.0423(T_{\mathrm{in}} - T_{\mathrm{eq}})], \quad (5)$$

where $\mathrm{pCO_{2_{in}}}$ is the temperature-corrected partial pressure of CO_2, $\mathrm{pCO_{2_{eq}}}$ is the observed partial pressure of CO_2, T_{in} is seawater temperature measured close to the inlet, and T_{eq} is the temperature measured in the tubing right before the equilibration chamber. This correction is, however, applied only since the beginning of August 2017, after the installation of the inlet thermometer measuring T_{in}. Additionally, sea bottom temperature below the inlet is monitored using another thermometer.

The atmospheric concentration of CO_2 at the height of 57 m was measured at the ICOS station (C in Fig. 1). At this station, the dry molar fraction of CO_2 is measured by using a very stable cavity ring-down spectroscopy technique (G2401, Picarro). For more information on the atmospheric ICOS measurements at Utö, the reader is referred to Kilkki et al. (2015).

3 Results and discussion

3.1 Suitability of the site for eddy covariance measurements

3.1.1 Environmental conditions

The measurement period (1 July – 1 November 2017) represents the late summer and autumn seasons of carbon cycle, when biological activity diminishes and the sea-air $\mathrm{pCO_2}$ difference shifts from negative to positive (Fig. 3e). At the beginning of this period, from July to mid-August, the atmospheric $\mathrm{pCO_2}$ exceeded that in the sea, and the sea acted as a sink of atmospheric CO_2. The average sea-air $\mathrm{pCO_2}$ difference from July to mid-August was 8.0 Pa. During the latter part of August, the sea turned to a source as a result of diminished primary production. The efflux was enhanced when thermal stratification broke down and

Atmos. Meas. Tech. Discuss., https://doi.org/10.5194/amt-2018-61
Manuscript under review for journal Atmos. Meas. Tech.
Discussion started: 19 April 2018

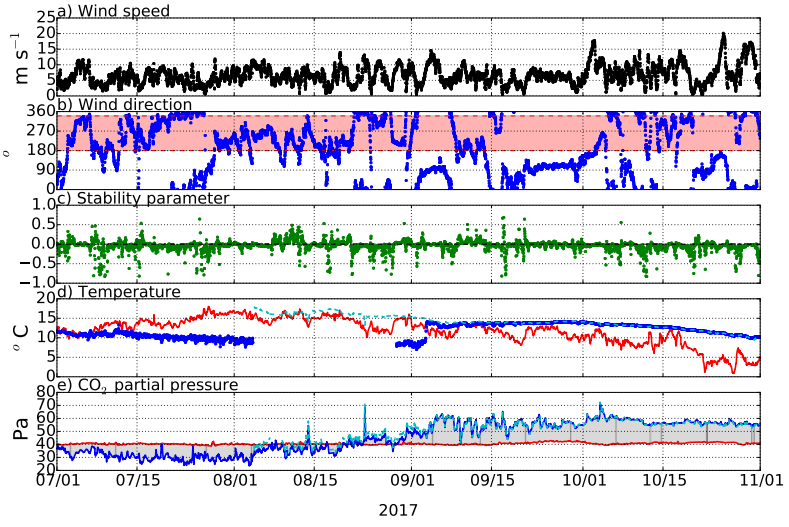

Figure 3. Environmental conditions at Utö in July–November 2017: (a) wind speed, (b) wind direction (red band indicates the directions suitable for sea-air flux measurements), (c) stability (z/L), (d) air temperature (red) and sea temperature at 5 m depth (cyan) and at the sea bottom (blue), and (e) CO_2 partial pressure in air (red), and temperature-corrected (cyan) and uncorrected (blue) CO_2 partial pressure in seawater at 5 m depth. Wind speed, wind direction, stability and air temperature were measured in the flux station (A in Fig. 1). Seawater temperatures and pCO_2 were measured at the inlet (B in Fig. 1). The pCO_2 in air was measured in the ICOS station (C in Fig 1).

CO_2-rich water surfaced at the beginning of September, resulting in increased surface pCO_2. After this event, the partial pressure difference stayed predominantly within 10–20 Pa for the rest of the measurement period, showing only occasional deviations from this range.

The values reported for the sea surface pCO_2 represent conditions at the depth of 5 m at a single point 250 m away from the flux tower, in the middle of the flux measurement sector. In some cases, this location may not represent the carbonate conditions of the whole sea sector area. Especially during the beginning of the measurement period, it is possible that there is horizontal differences in the surface pCO_2 due to variations in biological activity (Rutgersson et al., 2008). During other periods, the horizontal differences are likely to be small in the open sea areas and the surface sea layer is likely to be well-mixed at least to the depth of 5 m. Thus, we assume that our pCO_2 observations represent the surface conditions.

During our study period, the wind blew from the sea sector (180–340°) for 49 % of the time (Fig. 3). This caused gaps in the sea-air flux time series; for instance during the last two weeks of September, the wind directions were unsuitable for sea-air exchange measurements. The average wind speed within the marine wind sector was 6.9 $m\,s^{-1}$. Stability was mostly near-neutral. A small part (3.7 %) of the momentum fluxes measured in the marine sector were positive, and thus the corresponding CO_2 flux data were discarded.

Atmos. Meas. Tech. Discuss., https://doi.org/10.5194/amt-2018-61
Manuscript under review for journal Atmos. Meas. Tech.
Discussion started: 19 April 2018

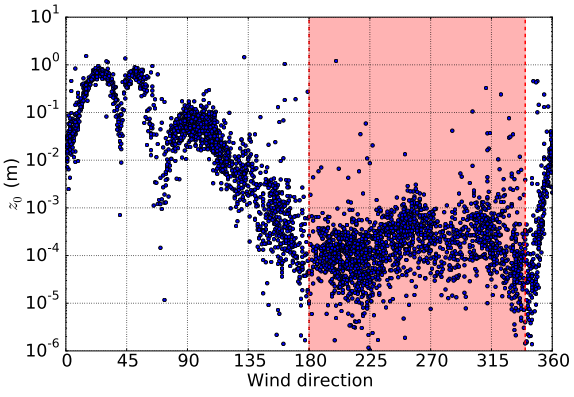

Figure 4. Surface roughness length as a function of wind direction. The red band indicates the directions considered the open sea sector.

In July, air temperature was still gradually increasing and it reached 18 °C by the end of the month. From the beginning of August, both air and sea surface temperature decreased approximately linearly. During the last three months, surface sea water cooled by 7 °C and air by 10 °C.

3.1.2 Horizontal homogeneity

Horizontal homogeneity within the sea sector (180–340°) was examined in terms of the surface roughness length (z_0), which was calculated from the logarithmic wind profile law using data collected during neutral conditions, $|z/L| < 0.01$ (Fig. 4).

The sea sector is clearly visible in a range of 180–340°, where z_0 is mainly lower than 1 mm. Outside this sector, z_0 is clearly higher, up to 1 m in northeastern wind directions. The sea sector indicated by z_0 coincides well with the sector deduced from the geographical map (Fig. 1).

While the sea sector can be considered sufficiently homogeneous, there is scatter in z_0 reflecting the fact that it depends on the sea state. Taylor and Yelland (2001) found that over a sea surface z_0 depends on the significant wave height and the slope of the wave. Since the measurement site is located on the coast, both the fetch and swell can depend on wind direction. Especially, a large swell can originate from the south, i.e. from the open waters of the Baltic Proper.

3.1.3 Spectral characteristics

The cospectra $Co_{w\mathrm{CO_2}}$ of both measurement setups agreed well with the modeled cospectrum in all frequencies (Fig. 5). The low frequency ends of the measured cospectra approach zero in a similar way to the modeled cospectrum.

The attenuation of the highest frequencies was slightly higher in the more complex tubing: $Co_{w\mathrm{CO_2}}$ of the test setup (with a drier and a virtual impactor) diverged from the modeled Co_{wT} at a slightly lower frequency than that of the standard setup. The half-power frequency for the standard and test system was 0.77 Hz and 0.59 Hz, respectively. These values were used to

Atmos. Meas. Tech. Discuss., https://doi.org/10.5194/amt-2018-61
Manuscript under review for journal Atmos. Meas. Tech.
Discussion started: 19 April 2018

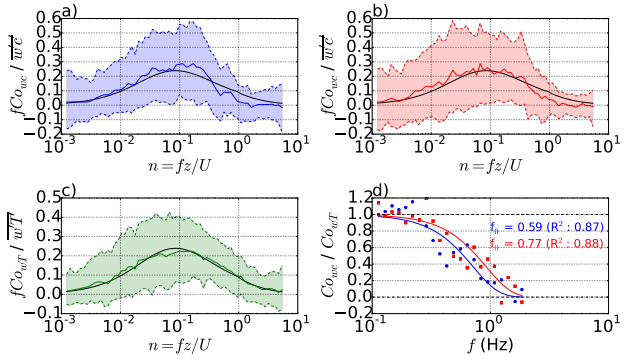

Figure 5. Cospectral densities $Co_{w\mathrm{CO_2}}$ of (a) the test setup and (b) the standard setup, and (c) Co_{wT}. The solid lines represent the mean cospectra and the dashed lines represent the 10th and 90th percentiles. The black line is the model Co_{wT} (Horst, 1997). (d) Ratios of cospectral densities (dots) and the fitted exponential transfer functions (solid lines), where the red color indicates the standard setup and the blue color indicates the test setup.

correct the CO_2 fluxes according to the model cospectrum. The high-frequency correction of the CO_2 flux during the typical meteorological conditions ($U = 6.9\,\mathrm{ms}^{-1}$ and $z/L = -0.05$) is 15 % for the test setup and 11 % for the standard setup.

The drier and virtual impactor added approximately 1 m to the length of tubing, which only has a minor effect on the attenuation of turbulent fluctuations. However, the virtual impactor forms a 90 ° angle to the tubing, which can stabilize the flow making it laminar at a higher Reynolds number, Re, than in a straight tube (Lenschow and Raupach, 1991). It would be ideal to have turbulent conditions in the tubes, because scalar fluctuations dampen less in a turbulent pipe flow due to the more uniform velocity profile (Lenschow and Raupach, 1991). At low temperatures (0 °C), Re of the standard setup was calculated to be 2980, whereas in the test setup it was 2380. By using the tube attenuation equations of turbulent flow presented by Massman and Ibrom (2008), the half-power frequencies were 13.7 and 7.2 Hz for the standard and test setup, respectively. Thus, at low temperatures, fluctuation attenuation due to transport in the tubes is not likely to affect the measurements. However, at higher temperatures (20 °C), the Reynolds number of the test setup (2100) falls into the laminar flow region, because kinematic viscosity increases with increasing temperature. By using the tube attenuation equations for laminar flow by Lenschow and Raupach (1991), the half-power frequency of the test setup at 20 °C was only 1.4 Hz, which is still higher than the empirically determined f_0.

The high frequency attenuation of H_2O signals of the standard setup was corrected in order to accurately compare the CO_2 flux measurements with different setups as a function of latent heat flux. The high frequency attenuation of H_2O flux of the standard setup was marked: f_0 ranged between 0.04 and 0.22 Hz, decreasing with increasing RH, which varied within 48–100 %. This attenuation is caused by sorption and desorption of water vapor at the walls of the tubings (Massman and Ibrom, 2008). During typical humidity conditions (RH = 80 %), the flux attenuation is 44 % of the real H_2O flux. The $Co_{w\mathrm{H_2O}}$ of the test setup was found to be distorted in all frequencies.

Atmos. Meas. Tech. Discuss., https://doi.org/10.5194/amt-2018-61
Manuscript under review for journal Atmos. Meas. Tech.
Discussion started: 19 April 2018

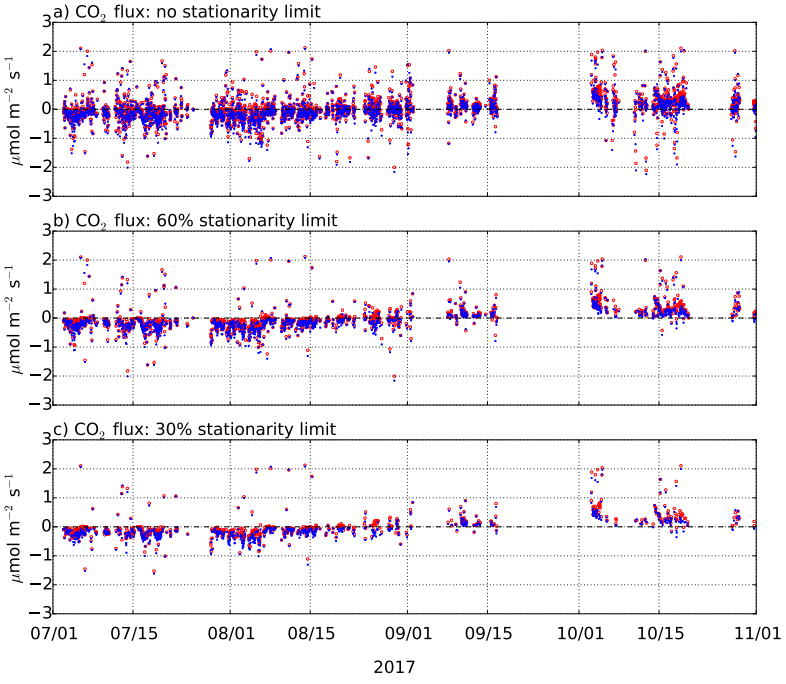

Figure 6. The effect of removal of non-stationarity cases on the CO_2 flux data: (a) no stationarity limit, (b) $RN_{\overline{w'c'}} < 0.6$ and (c) $RN_{\overline{w'c'}} < 0.3$. Red circle refers to the standard setup and blue dot to the test setup.

3.1.4 Stationarity

About half of the flow conditions for which the CO_2 flux was determined, 55 % for the standard setup and 63 % for the test setup, were found to be non-stationary, i.e. the difference between the 30 min flux and the mean of the corresponding 5 min fluxes exceeded 30%.

We found that this stationarity criterion removed unphysical values effectively (Fig. 6). During July, the partial pressure difference was negative (-9.3 Pa on average), and thus downward (negative) fluxes were expected. Relaxing the stationary limit from 30 % to 60 % had only a small effect on data filtering. If no stationarity limit was applied, 20 % and 25 % of CO_2 sea-air fluxes measured during July 2017 by the test and standard setup, respectively, were positive. By using the 60 % stationarity limit, only 5 % (test) and 6 % (standard) of the measured CO_2 fluxes were positive. With the 30 % stationarity limit, these numbers were only slightly lower, 3 % and 4 %, respectively.

Similarly high rejection rates have been obtained in previous studies. Miller et al. (2010) reported that 65 % of the sea-air CO_2 flux measurements failed a stationarity test in which the 13.7 min fluxes were compared with the averages of 3.4 min fluxes, and assumed that CO_2 concentration heterogeneity could be a reason for the high rejection rate. Likewise, Blomquist et al. (2014) concluded that horizontal CO_2 concentration gradients caused by continental pollution sources can reduce the

Atmos. Meas. Tech. Discuss., https://doi.org/10.5194/amt-2018-61
Manuscript under review for journal Atmos. Meas. Tech.
Discussion started: 19 April 2018

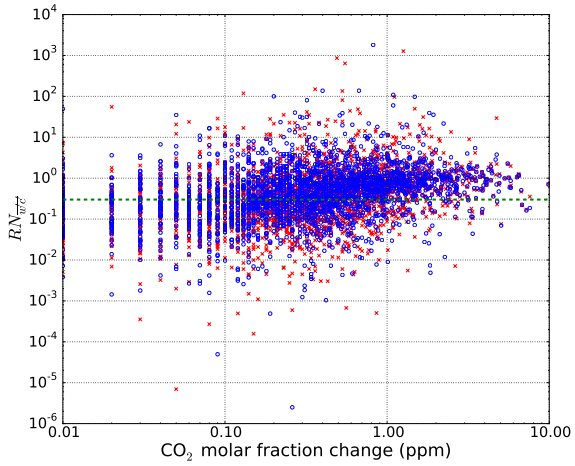

Figure 7. Relative non-stationarity of CO_2 flux as a function of the absolute change in CO_2 concentration during the averaging period: standard (red cross) and test (blue circle) setups. The green dashed line indicates the limit of $RN_{\overline{w'c'}} = 0.3$.

number of stationary situations. At Utö, concentration gradients may be produced by the horizontal heterogeneity due to the land-sea interface and the variations in marine primary production.

We examined how the absolute change in CO_2 concentration during the averaging period of 30 min relates to non-stationarity of CO_2 fluxes (Fig. 7b). The change in CO_2 concentration was calculated as a difference in the mean CO_2 molar fraction of the last 30 s and the first 30 s. Typically, a change larger than 1 ppm was associated with rejection of the measurement due to the non-stationarity of CO_2 flux. Only 14 % and 18 % of the sea-air CO_2 fluxes for the test and standard setup, respectively, passed the stationarity test with the 30 % limit, for the cases with a CO_2 concentration change larger than 1 ppm. For the cases where CO_2 concentration changed more than 2 ppm during the averaging period, only 5 % and 6 % of sea-air CO_2 fluxes passed this stationarity test.

If the time scale of the processes generating non-stationarity was less than the averaging time, it would be possible to reduce the amount of discarded non-stationary data by shortening the averaging time. To test for non-stationarity with shorter averaging periods, we calculated CO_2 fluxes for 15 min periods, which were compared with the average of 2.5 min CO_2 fluxes. It was found that this increased the number of accepted data only a little: by 6.1 % for the standard setup and 1.9 % for the test setup.

Even though a large number of the measurements did not meet the stationarity criterion ($RN_{\overline{w'c'}} < 0.3$), the occurrence of non-stationary conditions was temporally random, whereas unsuitable wind directions produced long continuous gaps in the measurement time series. For the calculation of a CO_2 budget, these gaps must be filled, for instance by using the measured pCO_2 difference and a gas transfer velocity parameterized as function of wind speed. Thus, continuous measurements of surface seawater and atmospheric CO_2 concentration provide useful additional data for a sea-air CO_2 flux station.

Atmos. Meas. Tech. Discuss., https://doi.org/10.5194/amt-2018-61
Manuscript under review for journal Atmos. Meas. Tech.
Discussion started: 19 April 2018

Atmospheric Measurement Techniques Discussions

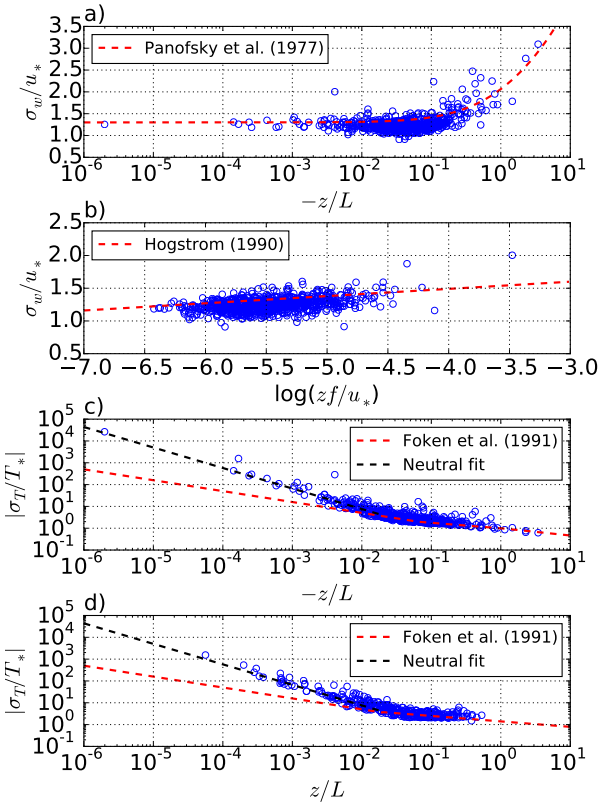

Figure 8. Integral turbulence characteristics. (a) σ_w/u_* as a function of stability parameter z/L, (b) σ_w/u_* as a function of zf_c/u_* and (c) σ_T/T_* as a function of z/L during unstable stability and (d) σ_T/T_* as a function of z/L during stable stability.

3.1.5 Turbulence

The Monin-Obukhov similarity theory predicts that statistical turbulence variables within the atmospheric surface layer are unique functions of the stability parameter (z/L), which combines information about the height above ground, surface shear stress, surface heat flux and buoyant processes. These so-called integral turbulence characteristics have been found to have the same stability dependence over the sea as on land (e.g. Smith and Anderson, 1984) and can be used to examine the development of turbulence.

Our data are in accordance with the results of Panofsky et al. (1977), who determined the relationship between the normalized standard deviation of vertical velocity and stability parameter:

$$\frac{\sigma_w}{u_*} = \alpha \cdot (1 - \beta \cdot z/L)^{1/3} \tag{6}$$

Atmos. Meas. Tech. Discuss., https://doi.org/10.5194/amt-2018-61
Manuscript under review for journal Atmos. Meas. Tech.
Discussion started: 19 April 2018

Atmospheric Measurement Techniques Discussions

where u_* is friction velocity, $\alpha = 1.3$ and $\beta = 3.0$. With large $-z/L$ values, the power law of 1/3 fits well to our observations, and the observed $\frac{\sigma_w}{u_*}$ approaches a constant of 1.3 in the neutral range similarly to Eq. 6. Most of the observations fall into the stability range between -0.1 and -0.01. Within this range, the observed $\frac{\sigma_w}{u_*}$ is mainly scattered between values 1.0 and 1.5.

However, Monin-Obukhov similarity theory does not consider all the necessary information for describing turbulence characteristics in all conditions; e.g. the effect of Coriolis and pressure-gradient forces are excluded. Högström (1990) showed that during neutral stratification $\frac{\sigma_w}{u_*}$ can be described with z, u_* and Coriolis parameter, f_c. Smedman (1990) found that this relationship is valid at widely differing sites, including both terrestrial and marine surfaces. Thus we tested our data with neutral stratification, $|z/L| < 0.1$, against the function proposed by Högström (1990):

$$\frac{\sigma_w}{u_*} = \gamma \cdot \log(z f_c / u_*) + \delta, \tag{7}$$

where $\gamma = 0.11$ and $\delta = 1.93$. This function provides a reasonable fit to our data and a better description of $\frac{\sigma_w}{u_*}$ in the stability range between -0.1 and -0.01 than Eq. 6 (Fig. 8).

For temperature, we compared the observations to the model of Foken et al. (1991):

$$\frac{\sigma_T}{T_*} = \begin{cases} 1.0 \cdot \left(\left|\frac{z}{L}\right|\right)^{-1/3} & , \quad \frac{z}{L} \leq -1 \\ 1.0 \cdot \left(\left|\frac{z}{L}\right|\right)^{-1/4} & , \quad -1 \leq \frac{z}{L} \leq -0.0625 \\ 0.5 \cdot \left(\left|\frac{z}{L}\right|\right)^{-1/2} & , \quad -0.0625 \leq \frac{z}{L} \leq 0.02 \\ 1.4 \cdot \left(\left|\frac{z}{L}\right|\right)^{-1/4} & , \quad \frac{z}{L} \geq 0.02 \end{cases} \tag{8}$$

Our observations were in accordance with the shape of this relationship, except for the near-neutral stability range, where the observations differ greatly from the model (Fig. 8c-d). As these cases have a very small sensible heat flux, $\frac{\sigma_T}{T_*}$ could be biased by division by a small number. However, this is not observed as the slope is well-organized and the spread is small. Our data suggest a steeper relationship should be used in this near-neutral stability range ($|z/L| < 0.02$):

$$\frac{\sigma_T}{T_*} = 0.1 \cdot \left(\left|\frac{z}{L}\right|\right)^{-0.94} \tag{9}$$

In the logarithmic scale, the slope (-0.94) in our fit is almost twice as steep as the corresponding slope determined by Foken et al. (1991), i.e. -0.5.

Overall, our observations were well organized as a function of stability parameter, or friction velocity in the neutral case, and thus we did not discard any of data based on the integral turbulence characteristics.

3.2 Setup comparison

The observed direction of the sea-air CO_2 fluxes was mainly consistent with the pCO_2 difference between the sea and the atmosphere, and both setups showed similar fluxes most of the time (Fig. 9). The standard setup tended to show slightly more positive fluxes than the test setup. In July, the pCO_2 difference was negative, and the mean sea-air CO_2 flux measured with the standard and test setup was -0.158 and -0.231 $\mu mol\, m^{-2}\, s^{-1}$, respectively. During the latter part of August (15–31

Atmos. Meas. Tech. Discuss., https://doi.org/10.5194/amt-2018-61
Manuscript under review for journal Atmos. Meas. Tech.
Discussion started: 19 April 2018

Atmospheric Measurement Techniques Discussions

August), when the pCO_2 difference was shifting from negative to positive, the mean flux measured with the standard system (0.003 $\mu mol\,m^{-2}\,s^{-1}$) was close to zero, while the test system still showed clearly negative fluxes (mean -0.082 $\mu mol\,m^{-2}\,s^{-1}$). During this period, the highest latent heat fluxes of the measurement period were measured, peaking at 274 $W\,m^{-2}$. During September, low latent heat fluxes (16 $W\,m^{-2}$ on average) were observed and both measurements showed the same mean monthly sea-air CO_2 flux: 0.180 $\mu mol\,m^{-2}\,s^{-1}$. The highest absolute monthly CO_2 fluxes were measured in October, when pCO_2 difference was continuously high (16.6 Pa on average) and wind speed peaked occasionally, resulting in monthly sea-air CO_2 flux averages of 0.364 and 0.301 $\mu mol\,m^{-2}\,s^{-1}$ by the standard and test setup, respectively.

There is limited amount of direct CO_2 flux measurements from this part of the Baltic Sea. The magnitude of the measured monthly sea-air CO_2 fluxes was of the same order as the modeled sea-air CO_2 fluxes in the Eastern Gotland basin (Norman et al., 2013). The modeled sink strength during the summer months was -0.1 $\mu mol\,m^{-2}\,s^{-1}$, whereas the measured flux was approximately twice as high in Utö in July. The shift from the negative to positive pCO_2 difference in Utö occurred two months before the corresponding shift in the model run.

The Nafion drier eliminated the water vapor fluctuations effectively. The latent heat flux (measured with the standard system) was mostly positive, ranging within -31–297 $W\,m^{-2}$, with an average of 53 $W\,m^{-2}$. The H_2O variance measured with the standard setup was 0.042 $mmol^2\,mol^{-2}$ on average, whereas the test setup measured the mean H_2O variance of 0.001 $mmol^2\,mol^{-2}$. Even though the Nafion drier in our setup did not remove water vapor completely, it attenuated the fluctuations at all frequencies, in the same way as the tubing of a closed-path system attenuates temperature fluctuations. Water vapor molar fraction measured by the test setup varied within 2.4–8.8 $mmol\,mol^{-1}$, whereas the standard setup showed water vapor values of 3.8–15.6 $mmol\,mol^{-1}$. Thus, a total removal of water vapor from the sample air is not required to eliminate the water vapor fluctuations.

A high correlation was found between the two measurement setups (Fig. 10). The Pearson product-moment correlation coefficient between the sea-air CO_2 fluxes measured by the setups was 0.96. During low latent heat fluxes (< 30 $W\,m^{-2}$), the correlation coefficient increased to 0.99. As latent heat flux increases, the standard setup shows more positive CO_2 fluxes than the test setup (Fig. 11). These results are in agreement with the conclusions of Landwehr et al. (2014), who found that during low latent heat fluxes the difference between the dried and undried sea-air CO_2 flux measurements were very similar, also proving that a Nafion drier (in our case combined with a virtual impactor) does not disturb the CO_2 flux measurements.

A comparison of the CO_2 flux difference as a function of latent heat flux shows that the error is negligible for very small latent heat fluxes (< 10 $W\,m^{-2}$). With high latent heat fluxes (~100 $W\,m^{-2}$), the mean difference is approximately 0.15 $\mu mol\,m^{-2}\,s^{-1}$. Since the sea-air fluxes of CO_2 are typically small, the effect of water vapor on CO_2 flux measurement can cause a change in its sign, as observed during the latter part of August. However, as the mean difference increases, also the scatter increases. There are only few data points with negative latent heat fluxes, so no conclusions can be drawn concerning the effect of negative water vapor fluxes on CO_2 fluxes.

We showed that the use of the combination of a virtual impactor and a Nafion drier did not disturb the measurement of CO_2 fluxes. Closed-path instruments are typically protected by one or two Teflon filters (one close to the inlet and another next to the instrument), which should prevent any liquid water from reaching the instrument. However, the use of a Teflon filter close

Atmos. Meas. Tech. Discuss., https://doi.org/10.5194/amt-2018-61
Manuscript under review for journal Atmos. Meas. Tech.
Discussion started: 19 April 2018

Atmospheric Measurement Techniques Discussions

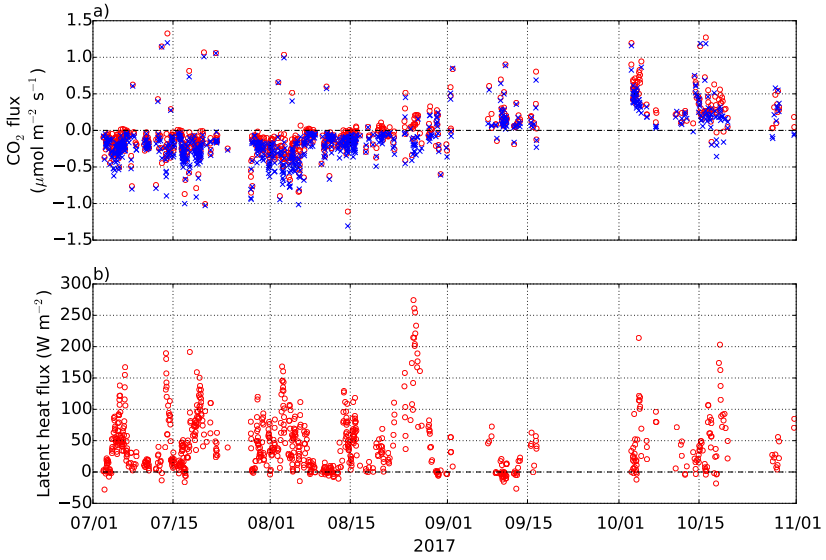

Figure 9. Sea-air fluxes of (a) CO_2 and (b) water vapor: standard setup (red circles) and test setup (blue crosses). Only the fluxes originating from the sea sector (Fig. 1) are shown.

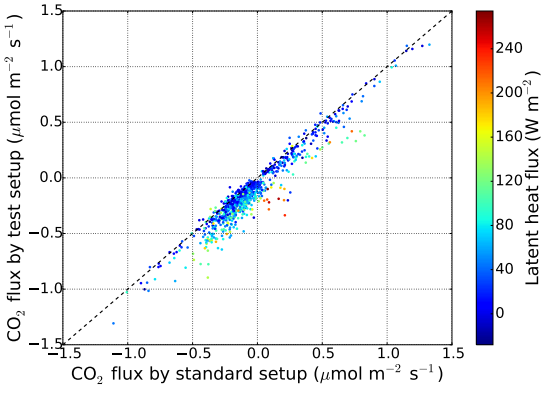

Figure 10. The sea-air CO_2 flux measured with the standard setup vs. the test setup (equipped with a drier and a virtual impactor). The marker color indicates the concurrent latent heat flux, and the dashed line represents the 1:1 relationship.

to the inlet may be unpractical, as a regular change of this filter may prove laborious. In such a case, we suggest a virtual impactor as an option for the protection of the instrument and the tubing from water and sea salt.

Atmos. Meas. Tech. Discuss., https://doi.org/10.5194/amt-2018-61
Manuscript under review for journal Atmos. Meas. Tech.
Discussion started: 19 April 2018

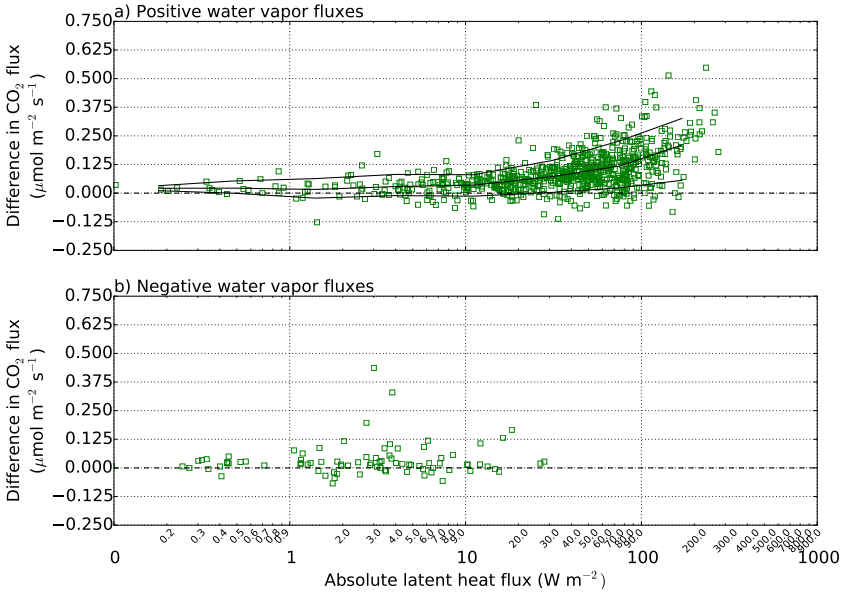

Figure 11. CO_2 flux difference as a function of latent heat flux (standard setup – test setup) for (a) positive and (b) negative water vapor fluxes. The lines show a fitted mean together with the 10th and 90th percentiles for eight logarithmically equally spaced bins.

4 Conclusions

In this paper, we presented new sea-air CO_2 flux measurements, comparing two closed-path gas analyzer setups installed on a shore of an island in the Baltic Sea. One of the setups was equipped with a drier and a virtual impactor. By inspecting several theoretical assumptions of the eddy covariance method, we showed that this land-based flux site is capable of effectively monitoring CO_2 fluxes between the atmosphere and the sea. The w-CO_2 cospectral densities calculated from our data showed an expected behavior with a moderate high frequency loss. Turbulence was well-developed, and the integral turbulence characteristics followed unique functions of stability and friction velocity.

We found that the two closed-path infrared gas analyzer setups showed similar CO_2 fluxes when latent heat fluxes were small. Correlation coefficient increased from 0.96 to 0.99 when only the CO_2 fluxes during small latent heat fluxes ($< 30\,\mathrm{W\,m^{-2}}$) were included. A higher latent heat flux resulted in a positive bias to the undried measurement. During high latent heat fluxes ($\sim 100\,\mathrm{W\,m^{-2}}$), the difference between the CO_2 flux measurements was $0.15\,\mu\mathrm{mol\,m^{-2}\,s^{-1}}$ on average, which is comparable to the monthly mean sea-air CO_2 flux. In July, the CO_2 partial pressure in the atmosphere exceeded that in the surface seawater, resulting in negative sea-air CO_2 fluxes, with monthly averages of -0.16 and $-0.23\,\mu\mathrm{mol\,m^{-2}\,s^{-1}}$ for the standard and test (drier) setup, respectively. In October, when the surface seawater had a higher CO_2 partial pressure than the atmosphere, the average sea-air CO_2 fluxes were 0.36 and $0.30\,\mu\mathrm{mol\,m^{-2}\,s^{-1}}$ for the standard setup and test setup, respectively.

Even though producing a high percentage of discarded observations (55–63 %), for high quality sea-air CO_2 flux measurements it is essential to reject non-stationary observations. If the non-stationary cases were not discarded, 20–25 % of the sea-air CO_2 fluxes in July had a wrong sign, whereas only 3–4 % of the measured fluxes had an unphysical direction if the non-stationary cases were rejected. This non-stationarity was found to be linked to the changes in atmospheric CO_2 concentration during the averaging period. A change larger than 2 ppm was associated with in the rejection rate of 94–95 % due to non-stationarity.

We showed that the use of the combination of a virtual impactor and a Nafion drier did not disturb the CO_2 flux measurement. While this configuration generated a slightly higher flux loss, we opt for this alternative for its reduced water vapour cross-sensitivity and better protection against sea spray.

Appendix A: Virtual impactor

The virtual impactor is based on two perpendicular air streams, which provides a means to separate particles by size (Fig. A1). The sample air stream is divided into minor and major flows : smaller particles are diverted to the major flow and large particles with higher inertia, in this case water droplets, continue to the minor flow. The 50 % cut-point of our virtual impactor was calculated to be 1.2–1.3 µm, i.e. a particle of this size has a 50 % probability of removal, while smaller particles are more likely to enter the major flow.

Competing interests. The authors declare that they have no conflict of interest.

Acknowledgements. This work was financially supported by the Finnish Meteorological Institute, the BONUS INTEGRAL project (BONUS Blue Baltic) and the JERICO-NEXT project (EU - Horizon 2020, 654410). The Integrated Carbon Observation System is acknowledged for providing the data of atmospheric CO_2 concentrations in Utö.

Atmos. Meas. Tech. Discuss., https://doi.org/10.5194/amt-2018-61
Manuscript under review for journal Atmos. Meas. Tech.
Discussion started: 19 April 2018

Atmospheric Measurement Techniques Discussions

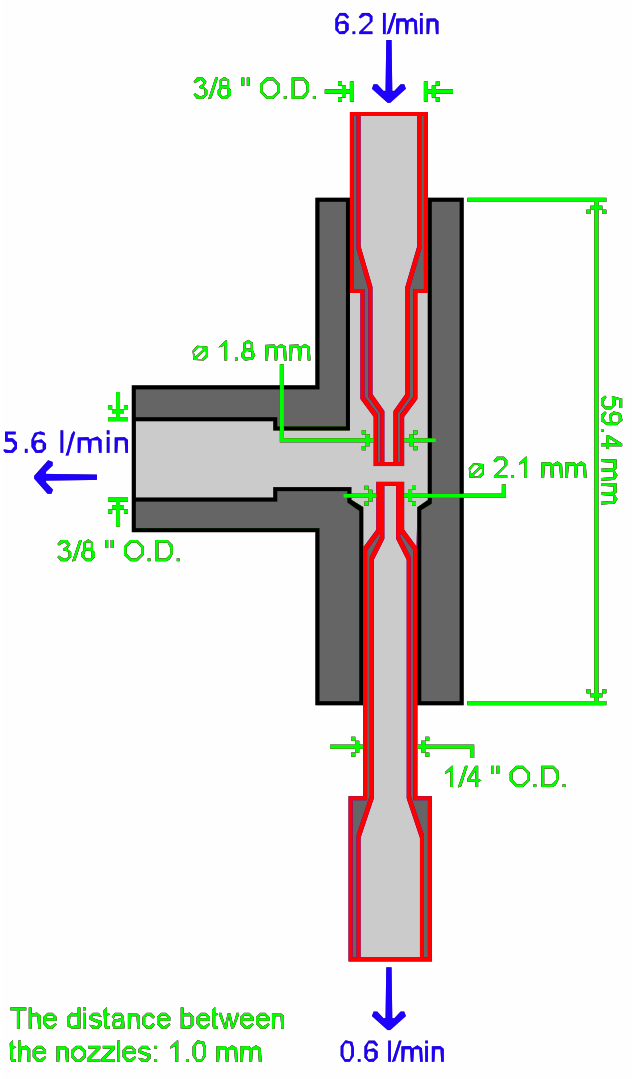

Figure A1. Schematics of the virtual impactor attached to the test setup. O.D. stands for outside diameter. The red pipes are enclosed by the black outer case. A more detailed figure is available on request.

References

Aurela, M., Lohila, A., Tuovinen, J.-P., Hatakka, J., Penttilä, T. and Laurila, T. Carbon dioxide and energy flux measurements in four northern-boreal ecosystems at Pallas. Boreal Environment Research 20:455–473. 2015.

Blomquist, B. W., B. J. Huebert, C. W. Fairall, L. Bariteau, J. B. Edson, J. E. Hare and W. R. McGillis. Advances in Air–Sea CO_2 Flux Measurement by Eddy Correlation. Boundary-Layer Meteorology 152:245—276. 2014.

Dabbert, W. F., D. H. Lenschow, T. W. Horst, P R. Zimmerman, S. P. Oncley and A. C. Delany. Atmosphere-surface exchange measurements. Science 260. 1993.

Edson, J.B., C. W. Fairall, L. Bariteau, C. J. Zappa, A. Cifuentes-Lorenzen, W. R. McGillis, S. Pezoa, J. E. Hare and D. Helmig. Direct covariance measurement of CO_2 gas transfer velocity during the 2008 Southern Ocean gas exchange experiment: wind speed dependency. Journal Of Geophysical Research 116. 2011.

Feely, R., S. Doney and S. Cooley. Ocean Acidication: Present Conditions and Future Changes in a High-CO_2 World. Oceanography 22(4):36–47. 2009.

Foken, T., G. Skeib and S. H. Richter. Dependence of the integral turbulence characteristics on the stability of stratification and their use for doppler-sodar measurements. Meteorologische Zeitschrift 41(4):311–315. 1991.

Foken, T. and B. Wichura. Tools for quality assessment of surface-based flux measurements. Agricultural and Forest Meteorology 78(1-2):83–105. 1996.

Heinze, C., S. Meyer, N. Goris, L. Anderson, R. R. Steinfeldt, N. Chang, C. Le Quere, and D. Bakker. The ocean carbon sink impacts, vulnerabilities and challenges. Earth System Dynamics 6:327-358. 2015.

Horst, T. W. A simple formula for attenuation of eddy fluxes measured with first-order response scalar sensors. Boundary-Layer Meteorology 82:219–233. 1997.

Högström, U. Analysis of turbulence structure in the surface layer with a modified similarity formulation for near neutral conditions. Journal Of the Atmospheric Sciences 47(16). 1990.

Ibrom, A., E. Dellwik, S. E. Larsen and K. Pilegaard. On the use of the Webb-Pearman-Leuning theory for closed-path eddy correlation measurements. Tellus Series B: Chemical and Physical Meteorology 59(5):937–946. 2007.

Jones, E. P. and S. D. Smith. A first measurement of sea-air CO_2 flux by eddy correlation. Journal Of Geophysical Research 82(37). 1977.

Kaimal, J. C., J. C. Wyngaard, Y. Izumi and O.R. Cote. Spectral characteristics of surface-layer turbulence. Quarterly Journal of the Royal Meteorological Society 98(417):563–589. 1972.

Kaimal, J. C. and J. J. Finnigan. Boundary layer flows - their structure and measurement. Oxford University Press. 1994.

Kilkki, J., T. Aalto, J. Hatakka, H. Portin and T. Laurila. Atmospheric CO_2 observations at Finnish urban and rural sites. Boreal Environmental Research 20:227–242. 2015.

Kohsiek, W. Water vapor cross-sensitivity of open path H_2O/CO_2 sensors. Journal of Atmospheric and Oceanic Technology 17(3):299–311. 2000.

Kondo, F. and O. Tsukamoto. Air-sea CO_2 flux by eddy covariance technique in the Equatorial Indian Ocean. Journal Of Oceanography 63:449–456. 2007.

Kondo, F., K. Ono, M. Mano, A. Miyata and O. Tsukamoto. Experimental evaluation of water vapour cross-sensitivity for accurate eddy covariance measurement of CO_2 flux using open-path CO_2/H_2O gas analysers. Tellus Series B: Chemical and Physical Meteorology 66(1). 2014.

Laakso, L., Mikkonen, S., Drebs, A., Karjalainen, A., Pirinen, P., and Alenius, P.: One hundred years of atmospheric and marine observations at Utö Island, the Baltic Sea, Ocean Sci. Discuss., https://doi.org/10.5194/os-2017-105, in review, 2018.

Lammert-Stockschlaeder, A. and F. Ament. CO_2-flux measurements above the Baltic Sea at two heights: flux gradients in the surface layer. Earth System Science Data 7:311–317. 2015.

Landwehr, S., S. D. Miller, M. J. Smith, E. S. Saltzman and B. Ward. Analysis of the PKT correction for direct CO_2 flux measurements over the ocean. Atmospheric Chemistry And Physics 14:3361–3372. 2014.

Lenschow, D. H. and M. R. Raupach. The attenuation of fluctuations in scalar concentrations through sampling tubes. Journal Of Geophysical Research. 96(D8):15259–15268. 1991.

Leuning, R. and K. M. King. Comparison of eddy-covariance measurements of CO_2 fluxes by open- and closed-path CO_2 analysers. Boundary-Layer Meteorology 59(3):297–311. 1992.

Mammarella, I., S. Launiainen, T. Gronholm, P. Keronen, J. Pumpanen, Ü. Rannik and T. Vesala. Relative humidity effect on high-frequency attenuation of water vapor flux measured by closed-path eddy covariance system. Journal Of Atmospheric And Oceanic Technology 26:1856-1866. 2009.

Massman W. J. and A. Ibrom. Attenuation of concentration fluctuations of water vapor and other trace gases in turbulent tube flow. Atmospheric Chemistry and Physics 8:6245–6259. 2008.

Miller, S. C., C. Marandino and E. S. Saltzman. Ship-based measurement of air-sea Co_2 exchange by eddy covariance. Journal Of Geophysical Research 115(D2). 2010.

Muller-Karger, F. E., R. Varela, R. Thunell, R. Luerssen, C. Hu and J. J. Walsh. The importance of continental margins in the global carbon cycle. Geophysical Research Letters 32(1). 2005.

Norman, M., A. Rutgersson and E. Sahlée. Impact of improved air-sea gas transfer velocity on fluxes and water chemistry in a Baltic Sea model. Journal of Marine Systems 111:175–188. 2013.

Panofsky, H. A., H. Tennekes, D. H. Lenschow and J. C. Wyngaard. The characteristics of turbulent velocity components in the surface layer under convective conditions. Boundary-Layer Meteorology 11:355–361. 1977.

Pirinen, P., H. Simola, J. Aalto, J.-P. Kaukoranta, P. Karlsson and R. Ruuhela. Tilastoja Suomen ilmastosta 1981–2010. 2012.

Prytherch, J., M. J. Yelland, R. W. Pascal, B. I. Moat, I. Skjelvan and C. C. Neill. Direct measurements of the CO_2 flux over the ocean: Development of a novel method. Geophysical Research Letters 37(3). 2010.

Rannik, Ü., T. Vesala and R. Keskinen. On the damping of temperature fluctuations in a circular tube relevant to the eddy covariance measurement technique. Journal Of Geophysical Research 102(D11):12789—12794. 1997.

Rutgersson, A., M. Norman, B. Schneider and H. Pettersson. The annual cycle of carbon dioxide and parameters influencing the air-sea carbon exchange in the Baltic Proper. Journal Of Marine Systems 74(1–2):381–394. 2008.

Sahlée, E., K. Kahma, H. Pettersson and W. Drennan. Damping of humidity fluctuations in a closed–path system. In Gas Transfer at Water Surfaces 6 (Eds. Komori S., McGillis W. and Kurose R.), Kyoto University Press, Kyoto, Japan, 516–523. 2011.

Smedman, A.-F. Some turbulence characteristics in stable atmospheric boundary layer flow. Journal Of The Atmospheric Sciences 48(6):856–868. 1990.

Smith, S. D. and R. J. Anderson. Spectra of humidity, temperature and wind over the sea at Sable Island, Nova Scotia. Journal Of Geophysical Research 89(C2):2029–2040. 1984.

Solomon, S., G.-K. Plattner, R. Knutti ja P. Friedlingstein. Irreversible climate change due to carbon dioxide emissions. Proceedings of the National Academy of Sciences of the United States of America 106(6): 1704–1709. 2009.

Takahashi, T., J. Olafsson, J. G. Goddard, D. W. Chipman and S. C. Sutherland. Seasonal variation of CO2 and nutrients in the high-latitude surface oceans: A comparative study. Global Biogeochemical Cycles 7(4):843—878. 1993.

Takahashi, T., S. C. Sutherland, C. Sweeney, A. Poisson, N. Metzl, B. Tilbrook, N. Bates, R. Wanninkhof, R. A. Feely, C. Sabine, J. Olafsson and Y. Nojiri. Global sea-air CO_2 flux based on climatological surface ocean pCO_2, and seasonal biological and temperature effects. Deep Sea Research II 49(2002):1601–1622. 2002.

Taylor, P. K. and M. J. Yelland. The dependence of sea surface roughness on the height and steepness of the waves. Journal Of Physical Oceanography 31. 2001.

Thomas, C. and T. Foken. Re-evaluation of Integral Turbulence Characteristics and their Parameterisations. In: 15th conference on turbulence and boundary layers, Wageningen, NL, 15–19 July 2002, American Meteorological Society, City, 129—132. 2002.

Webb, E. K., G. I. Pearman, and R. Leuning. Correction of flux measurements for density effects due to heat and water vapour transfer. Quarterly Journal of the Royal Meteorological Society 106(447):85–100. 1980.

Welp, L. R., R. F. Keeling, R. F. Weiss, W. Paplawsky and S. Heckman. Design and performance of a Nafion dryer for continuous operation at CO_2 and CH_4 air monitoring sites. Atmopsheric Measurement Techniques 6:1217–1226. 2013.

Wesslander, K. The carbon dioxide system in the Baltic Sea surface waters. Doctoral thesis. University of Gothenburg. 2011.

Yang, M., T. G. Bell, F. E. Hopkins, V. Kitidis, P. W. Cazenave, P. D. Nightingale, M. J. Yelland, R. W. Pascal, J. Prytherch, I. M. Brooks and T. J. Smyth. Air-sea fluxes of CO_2 and CH_4 from the Penlee Point Atmopsheric Observatory on the south-west coast of the UK. Atmopsheric Chemistry and Physics 16:5745–5761. 2016.